OBSERVATION OF FINE-ORDERED PATTERNS ON ELECTRODE SURFACES SUBJECTED TO EXTENSIVE EROSION IN A SPARK DISCHARGE

Moritz Wagner[1], Attila Kohut[2], Zsolt Geretovszky[2], Martin Seipenbusch[1,#], Gábor Galbács[3*]

[1] Institute for Mechanical Process Engineering and Mechanics, Karlsruhe Institute of Technology, Straße am Forum 8, D-76131 Karlsruhe, Germany

[2] Department of Optics and Quantum Electronics, University of Szeged, Dóm square 9, 6720 Szeged, Hungary

[3] Department of Inorganic and Analytical Chemistry, University of Szeged, Dóm square 7, 6720 Szeged, Hungary

*corresponding author

E-mail: galbx@chem.u-szeged.hu

#present address: Institute of Chemical Process Engineering, University of Stuttgart, Böblinger Str. 78, 70199 Stuttgart, Germany

1

ABSTRACT

This note describes the observation of pattern formation on the surface of metal electrodes used in a spark discharge. The spark discharge used in the experiments was a spark discharge generator (SDG) designed for the generation of nanoparticles. The generator was run in atmospheric pressure nitrogen flow, with the electrode gap adjusted to 3 mm. The spark repetition rate was about 30 Hz, at an average breakdown voltage of 6.6 kV. It was observed, that after extended duration (several hours) of sparking, the front face of the cylindrical electrodes exhibited an erosion pattern, which had a characteristic appearance both in the macro and micro dimensions. Apart from the expected rounding-off of the circular edge of the electrodes, the erosion pattern most often found consisted of a hexagonally ordered arrangement of protrusions on the surface. The ordered-protrusion/ordered-depression pattern occurred predominantly on initially cathodic electrodes and was discernible on copper, gold, nickel, silver and copper-nickel alloy electrodes. The topology of the erosion pattern and its time evolution was studied in detail on nickel electrodes by using optical microscopy and confocal laser scanning microscopy.

1. Introduction

Spark discharge plasma sources are widely used in diverse areas of science and technology. The numerous application fields include e.g. analytical atomic emission spectroscopy (Boumans, 1972; Zhou et al., 2005), electrical discharge machining (Ho & Newman, 2003), sintering of particulates (Mamedov, 2002), ignition of combustion engines, etc. only to name a few. In the past two decades, the spark discharge generator (SDG) also established itself as a distinguished physical method of nanoparticle (NP) generation, as it was realized that SDGs provide an exceptionally versatile, clean and efficient method of NP production (Schwyn et al., 1988; Byeon et al., 2008; Meuller et al., 2012; Hontañon et al., 2013; Pfeiffer et al., 2014). Spark discharges have been studied in a surprising detail over the past decades. Numerous excellent experimental and theoretical studies targeted the processes occurring in the spark gap (e.g. (Boumans, 1972; Meek, 1940; Walters, 1969)). Many fundamental phenomena have already been revealed, documented and discussed in the literature, such as streamer formation, sparking-off effects, rate of electrode material consumption, electrical and emission characteristics, etc. A relatively recent overview of the status of this productive field was provided by Bazelyan and Raizer (Bazelyan & Raizer, 1997). However, a detailed, high-resolution microscopy study of the eroded electrode surfaces subjected to extended sparking has not yet been reported in the literature.

In the present work, we describe the observation of fine (micro-scale) ordered erosion patterns on the surface of electrodes subjected to a large number of sparks. The conditions used in the experiments are typical of SDGs, that is the discharge is a high current oscillatory spark discharge, running in atmospheric pressure, flowing nitrogen gas. The research was carried out as part of the activities within the Buonapart-e project ("Better Upscaling and Optimization of Nanoparticle and Nanostructure Production by Means of Electrical Discharges", a research project funded by the European Union under No. 280765).

2. Material and methods

Electrodes were subjected to erosion caused by recurring spark discharges in nitrogen atmosphere at atmospheric pressure. Cylindrical electrodes made of pure nickel, gold, silver, copper and a number of copper-nickel alloys (ChemPUR GmbH, Germany) with a diameter of 3 mm were positioned axially, at a distance (electrode gap) of 3 mm. All electrode materials were of at least 99.95% purity, while the oxygen content of the nitrogen gas was minimized using an oxygen trap. Both the SDG housing, as well as all tubings were made of stainless steel vacuum-tight components (ISO KF and Swagelok connectors). The geometry of the SDG chamber was the "traditional" 4-way cross design. Before each experimental run, the setup was evacuated to a pressure of below 1 mbar using a rotary vane pump (Pfeiffer Vacuum Duo 10M) and subsequently filled with nitrogen of 99.999% purity, which was purified further using an oxygen trap (Air Liquide O_2-Free). During the experiments, the SDG housing was flushed with 4 slm of atmospheric pressure nitrogen. The flow of nitrogen was controlled by a mass flow controller (MKS 1079A), and the pressure of the gas was continuously monitored by using an electronic vacuum gauge (Thyracont VSC43).

The circuit consisted of a capacitor charging high voltage power supply (CCR20-N-300, Technix) connected to an oil-polymer capacitor (Type 440PM815, General Atomics) with a capacitance of 15 nF. The spark gap was directly connected to the capacitor. The discharge frequency and energy of the sparks were governed by the breakdown voltage of the gas in the gap. The high voltage power supply was set to deliver a 3 mA charging current, which resulted in an oscillating discharge with a frequency of about 30 Hz at an average breakdown voltage of 6.6 kV. Each experimental run consisted of about 4 hours of erosion, equivalent to approximately $4 \cdot 10^5$ sparks with an average energy stored in the capacitor of about 330 mJ. After each run, the changes occurring on the surface of the electrode tips were documented using optical and confocal laser scanning microscopy (CLSM) (Keyence VK-X100K). Each electrode was subjected to several experimental runs in order to identify temporal changes in electrode surface morphology (up to a total of 20 hours duration). Throughout this report, the electrodes are referred to as initially cathodic or initially anodic, referring to the polarity of the electrode at the onset of the oscillating discharge.

3. Results

It was observed, that after extended duration sparking, the tip of both electrodes exhibited an erosion, which had a characteristic appearance both in the macro and micro dimensions. At the macro level, the erosion-affected area extended beyond the face of the cylindrical electrode, i.e. a ring of ca. 2 mm width along the side of the circular front face of the electrode also exhibited erosion. In long-term experiments, the overall shape of the initially cathodic electrode always converged towards a rounded-off shape (a hemisphere-like shape). At the same time, the initially anodic electrode was often found to exhibit a large central concave part (intrusion).

At the micro level, all spark-affected areas were covered by ordered, small diameter, circular protrusions. The patterns appeared to be consistent in their configuration, even after several subsequent experimental runs. Patterns were detected on electrodes from a number of metals and were found to be material-dependent both in their appearance and morphology. Some examples can be seen in Fig 1.
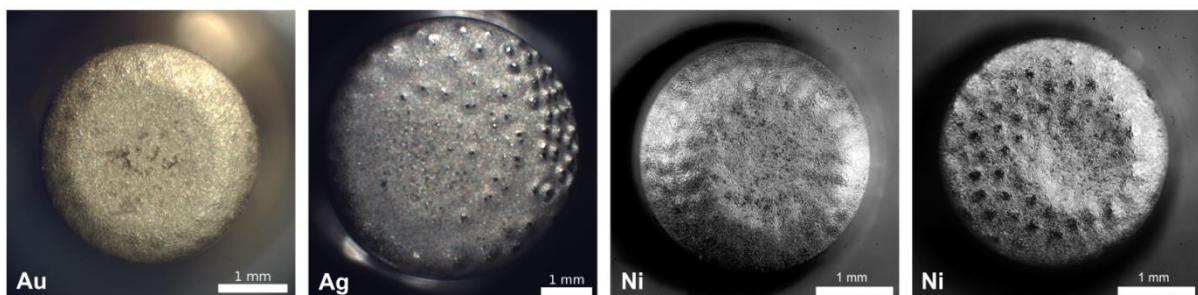

Figure 1. Optical micrographs of the erosion at initially cathodic Au, anodic Ag, cathodic Ni and anodic Ni electrode front surfaces after prolonged sparking (ca. $2.4 \cdot 10^{6}$ sparks).

The erosion pattern most often found consisted of a more or less symmetrycal, closely packed ordered arrangement of protrusions on the surface. This pattern occurred predominantly on initially cathodic electrodes and was discernible on copper, gold, nickel, silver and copper-nickel alloy electrodes. The characteristic peak-to-peak distance of this pattern was found to be around 250 to 300 µm (see Fig 2. for data obtained with Ni electrodes by confocal laser scanning), practically independent of the electrode material and polarity. As nickel electrodes were found to show the most corrugation, quantitative experimental data was mainly collected with Ni electrodes in the present study.
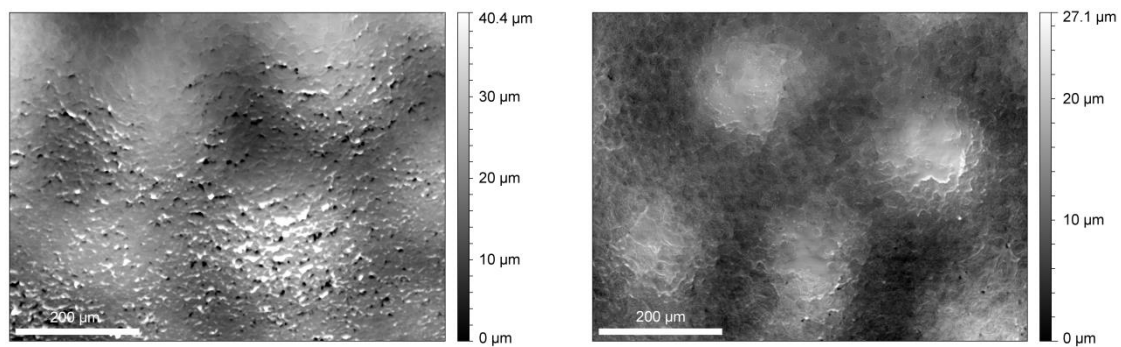
Figure 2. Confocal laser scanning height maps of patterns found on Ni electrode front surfaces of initially cathodic (left) and anodic (right) polarity after ca. $2.4 \cdot 10^6$ sparks. Macro-scale surface curvature has been corrected for in the images.

Using Ni electrodes, the time evolution of the mean distance from protrusion center to protrusion center ("peak-to-peak" distance) and the height of the protrusions (with reference to the "valley") were also studied. In these experiments, the sparking was interrupted at 4-hour intervals (after ca. $5 \cdot 10^5$ sparks) in order to take out the electrodes and subject them to laser confocal scanning microscopy. The electrodes were then placed back into the SDG and the sparking was continued. Special care was taken during electrode placement so that the electrodes were in identical position during each experimental run. The data in Fig 3. reveal that the peak-to-peak distance remains consistent once the pattern has been formed. The electrode polarity also does not seem to possess a strong influence on the lateral dimensions of the pattern. The height of protrusions was found to increase with the duration of sparking and to depend on the electrode material. During the first ten hours of erosion, the pattern became better defined. After this initial period, the pattern appeared to be fairly consistent, as the average peak height remained the same, even after very long erosion times (up to 20 hours). The final mean height of the protrusions on the initially cathodic electrode was about 1.5 times larger than that of the initially anodic electrode.
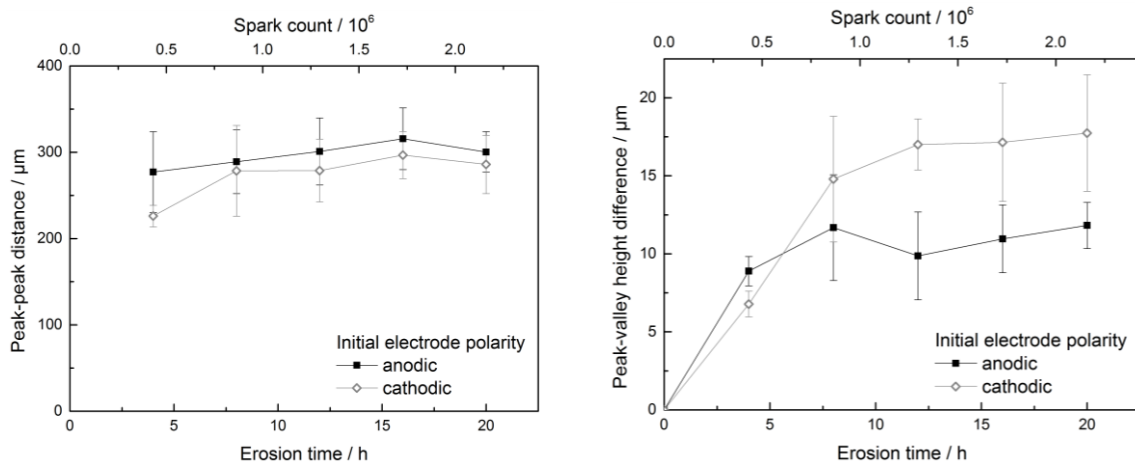
Figure 3. The time evolution of the peak-to-peak distance (left) and peak height (right) of protrusions on a pair of Ni electrodes as obtained by CLSM measurements. Each data point in the graphs represent the mean of at least ten measurements on the CLSM map, with the standard deviation indicated as an error bar.

A metallographic analysis of the cross-section of a copper-nickel alloy electrode with the erosion pattern was also performed by optical microscopy on a polished and etched axial cross-section of the electrode. This analysis showed that crystallites are smaller than 50 μm, which is significantly smaller than the characteristic lateral dimension of protrusions and no correlation was found between the arrangement of protrusions and the crystalline structure of the electrode.

4. Discussion

The formation of patterns on surfaces subjected to electrical discharges has been reported for glow discharges (GD), arc discharges and dielectric barrier discharges (DBD) (Astrov et al., 1996; Gurevich et al., 2003; Trelles, 2013, Hontañon 2014). A considerable amount of work towards the modelling of pattern formation can also be found in the literature, with regard to both for the generalized process (Cross & Hohenberg, 1993; Turing, 1952) as well as for certain special electrical discharges (Almeida & Benilov, 2013; Müller, 1988, Trelles 2014). The patterns described therein are diverse and comprise regular arrangements of dots (Astrov et al., 1996), lines (Ammelt et al. 1997) and concentric circles (Gurevich et al., 2003). As it has been pointed out by Benilov in his recent review (Benilov 2014), regular patterns of multiple spots, such as those found on the electrodes of certain glow discharges and

7

ambient-gas arcs, corona discharges and dielectric barrier discharges, are produced by self-organization. The theoretical approach to the physical explanation of these patterns in the literature is either *a)* phenomenological simulation based on an assumption that the distribution of parameters across the electrode surface are governed by reaction–diffusion equations (e.g. Astrov 1996, Gurevich 2003, Müller 1998), or *b)* first-principle modeling of gas discharges (e.g. Almeida & Benilov 2013, Trelles 2013, Trelles 2014). Trelles has recently reported about non-LTE simulation results for arc discharges in the pin cathode - plane anode configuration (Trelles 2014) and found that the anode pattern formation is strongly affected by the current as well as the anode cooling. The number, size and location of the spots was found to be markedly current-dependent. An increasing lack of symmetry in the arrangement of spots was observed for decreasing currents and increasing cooling. Trelles suggested that the pattern formation is due to an imbalance between the heat lost by the heavy species to the electrode and current transfer by electrons. It was also stated that the presence of competing processes is a common characteristic of self-organization phenomena (Benilov 2014, Trelles 2014). Recently a cluster issue of Plasma Source Science and Technology was specifically dedicated to the topic of 'Spots and patterns on electrodes of gas discharges' (Volume 23, Issue 5, October 2014). However, to the knowledge of the present authors, no report has been made in the literature before the present work on the observation of erosion pattern formation in spark discharges.

While the electrode surface patterns described in this report bear striking resemblance to those found in arc and glow discharges, their formation can not be simply explained by the same processes, however there are similarities. In contrast to other discharges, the spark discharge in an SDG is a highly localized and transient phenomenon. The direction and intensity of the current is rapidly changing and the electrodes typically have identical shape and an axi-symmetric arrangement. Each and every spark only affects a part of the electrode surface, as is obvious from the substantial difference between the diameter of the spark channel and that of the electrode (e.g. (Bazelyan & Raizer, 1997, Palomares 2015)). The fact that the electrode pattern begins to emerge only after a large number (10^5 to 10^6) of spark events also suggests that each spark event only contributes a small part of the whole pattern. The observed annular erosion of the electrodes is most probably the result of many localized erosion events hitting the front surface of the electrode near the rim. In can also be added that our observations are in line with the results of Trelles obtained for arc discharges

and described above. In an SDG setup, the peak current is very high (500 to 1000 A) and there is no water cooling applied to the electrodes, hence a very consistent spot pattern can be expected. Nevertheless, it is assumed that the pattern retains a dynamic nature due to the highly transient currents.

Since we observed pattern formation on various metallic electrode materials, patterning clearly seems to be a general phenomenon in spark erosion. This is also supported by the fact that the ordered-protrusion patterns on all materials shared the same characteristic peak-to-peak distance as well as that no correlation was found between the crystal structure and the surface pattern. The geometrical dimensions of the pattern hence seem to be governed by experimental factors other than the electrode material.

The existence of a plateau in the time evolution of the height of protrusions indicates that there are at least two competing processes at work, as is typical of other pattern-forming mechanisms (Turing, 1952; Radehaus et al., 1992, Benilov 2014, Trelles 2014). Tentatively said, the first process activates the formation of protrusions by preferential erosion, while a second one has an inhibitory or stabilizing effect in that it keeps the height difference between protrusions and valleys from increasing beyond a certain limit.

The small surface area affected by a single discharge channel, together with a large number of sparks needed for the formation of a coherent, regular pattern necessitates the interaction between subsequent sparks. It is known that for a short period of time, up to about 100 ms, after a pulsed arc or spark discharge event, the breakdown voltage of a subsequent discharge event is significantly reduced as compared to a static breakdown. This phenomenon is known as gap recovery. At a discharge frequency of 30 Hz, the average time between two consecutive sparks is about 33 ms, which is within the time frame for gap recovery data found in the spark discharge literature (Crawford & Edels, 1960; Shaw & Whittaker, 1964). Gap recovery was reported to be influenced by a number of parameters, including gas pressure, gas flow, gap width, and electrode material. We therefore assume that spark interaction caused by incomplete spark gap recovery is one of the processes behind pattern formation.

Further, detailed experiments are needed to reveal the influence of experimental parameters on the electrode patterns. Such experiments are under execution in our laboratory.

References

Almeida, P. G. C., & Benilov, M. S. (2013). Multiple solutions in the theory of direct current glow discharges: effect of plasma chemistry and nonlocality, different plasma-producing gases, and 3D Modelling. Physics of Plasmas, 20, 101613.

Ammelt, E., Astrov, Yu., & Purwins, H-G. (1997). Stripe turing structures in a two-dimensional gas discharge system. Physical Review E, 55, 6731–6740.

Astrov, Yu., Ammelt, E., Teperick, S. & Purwins, H-G. (1996). Hexagon and stripe turing structures in a gas discharge system. Physics Letters A, 211, 184–190.

Bazelyan, E. M. & Raizer, Y. P. (1997). Spark Discharge. Boca Raton: CRC Press.

Benilov, M. S. (2014). Multiple solutions in the theory of dc glow discharges and cathodic part of arc discharges. Application of these solutions to the modeling of cathode spots and patterns: a review, Plasma Sources Science and Technology, 23, 054019.

Boumans, P. W. J. M. (1972). Excitation of spectra. In E. L. Grove (Ed), Analytical Emission Spectroscopy. New York: Marcel Dekker.

Byeon, J. H., Park, J. H., & Hwang, J. (2008). Spark generation of monometallic and bimetallic aerosol nanoparticles. Journal of Aerosol Science, 39, 888-896.

Crawford, F. W., & Edels, H. (1960). The reignition voltage characteristics of freely recovering arcs. Proceedings of the IEEE, 107, 202-212.

Cross, M. C., & Hohenberg, P. C. (1993). Pattern formation outside of equilibrium. Reviews of Modern Physics, 65, 851-1112.

Gurevich, E., Zanin, A., Moskalenko, A., & Purwins, H-G. (2003). Concentric-ring patterns in a dielectric barrier discharge system. Physical Review Letter, 91, 154501.

Ho, K. H., & Newman, S. T. (2003). State of the art electrical discharge machining (EDM). International Journal of Machine Tools and Manufacture, 43, 1287–1300.

Hontañon, E., Palomares, J. M., Stein, M., Guo, X., Engeln, R., Nirschl, H., & Kruis, F. E. (2013). The transition from spark to arc discharge and its implications with respect to nanoparticle production. Journal of Nanoparticle Research, 15, 1957.

Hontañon, E., Palomares, J. M., Stein, M., Guo, X., Engeln, R., Nirschl, H., & Kruis, F. E. (2014). Influence of the inter-electrode distance on the production of nanoparticles by means of atmospheric pressure inert gas dc glow discharge. Journal of Physics D, 47, 415201.

Palomares, J. M., Kohut, A., Galbács, G., Engeln, R., Geretovszky Zs. (2015) A time-resolved imaging and electrical study on the operation of a high current atmospheric pressure spark discharge. Journal of Applied Physics, submitted.

Mamedov, V. (2002). Spark plasma sintering as advanced PM sintering method. Powder Metallurgy, 45, 322-328.

Meek, J. M. (1940). A theory of spark discharge. Physical Review, 57, 722-727.

Meuller, B. O., Messing, M. E., Engberg, D. L. J., Jansson, A. M., Johansson, L. I. M., Norlén, S. M., Tureson, N., & Deppert, K. (2012). Review of spark discharge generators for production of nanoparticle aerosols. Aerosol Science and Technology, 46, 1256-1270.

Müller, K. G. (1988). Structures at the electrodes of gas discharges. Physical Review A, 37, 4836-4845.

Pfeiffer, T. V., Feng, J., & Schmidt-Ott, A. (2014). New developments in spark production of nanoparticles. Advanced Powder Technology, 25, 56-70.

Radehaus, C., Willebrand, H., Dohmen, R., Niedernostheide, F-J., Bengel, G., & Purwins, H-G. (1992). Spatially periodic patterns in a DC gas-discharge system. Physical Review A, 45, 2546-2557.

Schwyn, T. V., Garwin, E., & Schmidt-Ott, A. (1988). Aerosol generation by spark discharge. Journal of Aerosol Science, 19, 639-642.

Shaw, A. B. and Whittaker, D. (1964). Effect of gas flow on post-arc gap recovery. Proceedings of the IEEE, 111, 193-202.

Trelles, J. P. (2013). Formation of self-organized anode patterns in arc discharge simulations. Plasma Sources Science and Technology, 22, 25017.

Trelles, J.P. (2014). Electrode patterns in arc discharge simulations: effect of anode cooling. Plasma Sources Science and Technology, 23, 054002

Turing, A. M. (1952). The chemical basis of morphogenesis. Philosophical Transactions of the Royal Society B, 237, 37–72.

Walters, J. P. (1969). Historical advances in spark emission spectroscopy. Applied Spectroscopy, 23 317-331.

Zhou, Z., Zhou, K., Hou, X., & Luo, H. (2005). Arc/spark optical emission spectrometry: principles, instrumentation, and recent applications. Applied Spectroscopy Reviews, 40, 165-185.